Communication

Passive Beam-Steering Gravitational Liquid Antennas

Chaoyun Song, Elliot L. Bennett, Jianliang Xiao, Tianyuan Jia, Rui Pei, Kwai-Man Luk, and Yi Huang

Abstract— We present a new concept to passively steer the antenna radiation beam to a fixed direction by utilizing the liquid fluidity behavior due to gravity. Completely different from existing technologies, the proposed antenna does not require any additional mechanical structures, phase shifting circuitry, liquid pumps, tunable elements, or their associated components. By properly designing the structure and resonant mode of the liquid dielectric resonator, the proposed passive antenna can automatically steer the radiation beam to the fixed and desired direction for communication upon physical reorientation of the antenna. An antenna prototype has been proposed with a fundamental resonant band of 1.4–1.8 GHz by using new liquid materials, while its passive beam-steering feature has been experimentally verified. This simple, elegant, and low-cost antenna has combined the gyroscopic correction, gravity, and beam steering into one for the first time, presenting significant implications for radio communications and radar systems that demand an adaptive antenna beam in certain directions.

Index Terms— Beam steering, dielectric resonator antenna (DRA), liquid antennas, passive antennas, wideband antennas.

I. INTRODUCTION

Antenna beam steering is an advanced technology for radio communications and radar applications and is realized by using mechanical or electrical methods. Mechanical beam steering is relatively slow and has only found limited applications, e.g., air traffic control. In contrast, electronic beam steering can be much faster and provide more functions than mechanical steering, and it has now been widely applied to commercial and military applications. State-of-the-art beam-steering antennas and arrays typically comprise a number of elements arranged in a specific pattern whose radiation amplitude and phase can be controlled in order to steer the main radiation lobe in a certain direction [1]–[3]. The phase shift is achieved through the use of either analog or digital electronic phase shifters [4], [5]. Conventional analog phase shifters are typically constructed using tunable elements, such as semiconductor varactor diodes [6], MEMS varactors [7], or a tunable dielectric capacitor [8]. Semiconductor varactor diodes can provide relatively fast switching times, but they tend to become very lossy as the frequency increases (i.e., >10 GHz). MEMS varactors have a lower loss, but they could have a relatively poor power handling capability. Moreover, the aforementioned state-of-the-art beam-steering antennas and arrays employ relatively complex electronic phase shifting circuitry. The size of the complete antenna system can be very large, especially if it is used for satellite communication applications. Therefore,

further miniaturization and simplification of beam-steering antennas have been an open challenge for decades [8].

The use of liquids, e.g., liquid metal and dielectric fluids, to develop and produce antennas has become possible in the recent years [9], [10]. There are at least two advantages in replacing traditional metals with novel liquid materials. First, there is an increasing demand for reconfigurable and flexible antennas for emerging and future industrial applications. Second, small, conformal, and/or transparent antennas are needed for a range of commercial [e.g., 5G mobile communications, body area networks, and Internet of Things (IoT)] and military (e.g., soldiers, ships, and vehicles) applications [11]. In addition to liquid metal materials, such as eutectic gallium–indium (EGaIn), dielectric fluids, such as deionized water, organic solvents, and ionic liquids, can also be used as the radiating element in antenna designs. For example, water antennas can significantly reduce the electrical size of the device compared with traditional metal-based antennas due to the high relative dielectric constant of water (∼78) [12]–[14]. However, water-based antennas have some drawbacks, such as relatively low radiation efficiency in high-frequency bands (due to a large dielectric loss tangent), temperature-dependent performance, and phase changes such as evaporation or freezing. To address these drawbacks, some dielectric solvents have been selected for use in place of water, due to their much smaller loss tangent, stable dielectric relaxation, and lower freezing point [15], [16]. However, there are still problems with such solvent-based liquid antennas. For example, most organic solvents are flammable and with high vapor pressures, resulting in high evaporation rates and potential safety concerns [17]. Thus, there is a need to use liquid materials with more stable and safer material properties. In addition, current reconfigurable liquid antennas are typically based on a pump system to control the liquid flow and thereby tuning the device structure [16]. In this scenario, the pump itself requires an electrical power supply and a space for its installation on the antenna system, which is not desirable. There is a need for reconfigurable, beam-steering antenna with greatly improved operating characteristics and much-reduced cost and complexity, while circumventing the aforementioned shortcomings.

In this Communication, we demonstrate a novel passive beam-steering liquid antenna system without the need for pumps, electronic phase shifting circuitry, and associated power supply. The beam-steering feature is achieved by controlling the variation of the antenna radiation mode originating from the biphasic liquid fluidity behavior due to gravity. The radiation beam of the proposed antenna can be automatically steered/tilted to the target direction upon dynamic physical movement of the antenna. As an example, we propose an antenna prototype which operates at GPS bands for satellite communications. Using the nature of gravitational force itself to automatically steer the antenna beam, our liquid antenna is truly passive, with no electrical power required, and has significant advantages over traditional electrical beam-steering antenna arrays in terms of cost, compactness and simplicity.

The rest of this Communication is organized as follows. The antenna geometry and operating mechanism are introduced in Section II. The liquid material characterization is presented in
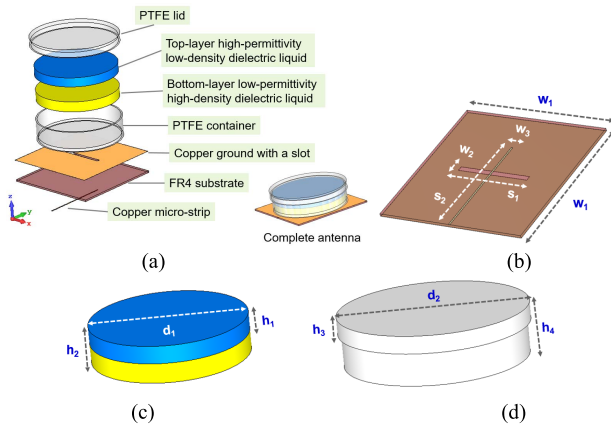
Fig. 1. (a) Materials and overall assembly of the proposed liquid antenna. Detailed dimensions of (b) PCB (FR4 substrate $\varepsilon_r = 4.5$, thickness = 1.6 mm). (c) Two layers of liquid resonators. (d) Liquid container and lid (made of PTFE, $\varepsilon_r = 2.1$, thickness = 2 mm). The size of the PCB is $w_1 \times w_1$ = 100 × 100 mm², S_2 = 65 mm, w_3 = 1 mm, S_1 = 44 mm, w_2 = 3 mm, d_1 = 79 mm, h_2 = 19 mm, h_1 = 9.5 mm, d_2 = 84 mm, h_4 = 23 mm, and h_3 = 8 mm.

Section III. The antenna performance validations and discussions are given in Sections IV. Finally, conclusions are drawn in Section V.

II. DEVICE STRUCTURE AND MECHANISM

A. Antenna Structure

Fig. 1(a) depicts the materials and overall assembly of the proposed liquid antenna. It is noted that the antenna consists of two different layers of dielectric liquids (with extremely low electrical conductivity) that act as the main radiator. Notably, the first liquid and the second liquid must be immiscible and must not chemically react with each other (e.g., water and oil). Moreover, the liquid on the top layer must also have a higher relative permittivity and lower density than the liquid on the bottom layer. Both liquids are contained within a cylinder-shaped container and screw-threaded lid. A ground plane is placed below the liquid produced on the PCB ground. The detailed geometry and dimensions of this proposed antenna are given in Fig. 1(b)–(d).

The radiation mechanism of the proposed liquid antenna is achieved by feeding the microstrip and aperture slot. In this case, the feed aperture will be excited like a magnetic dipole. The electric field of the magnetic dipole will be further amplified by the dielectric liquid resonators above the slot, thus producing the desired electromagnetic radiation. Such a radiation scheme is similar to that of a dielectric resonator antenna (DRA) [18]. In principle, different resonant modes with a variety of radiation patterns and beam directions can be generated by using dielectric resonators with different shapes and feeding schemes. However, in practice, it is relatively difficult to change the shape of the conventional DRAs as they are typically made of solid materials, such as glass and ceramics. The liquid resonator structure of the proposed design would vary upon physical reorientation of the device itself, such as tilting or flipping. This is due to the nature of the immiscible liquids with vastly different densities, resulting in reordering in relation to gravity. Such structural variations will consequently change the resonant mode and radiation pattern of the antenna. Beam-steering/switching features of the antenna can be realized by taking advantage of this phenomenon and proper control of the resonant mode.

B. Pros and Cons of This Work

To better understand the advancement brought about by the proposed passive beam-steering antenna, an example of the antenna employed in a vehicle-mounted satellite communication system is
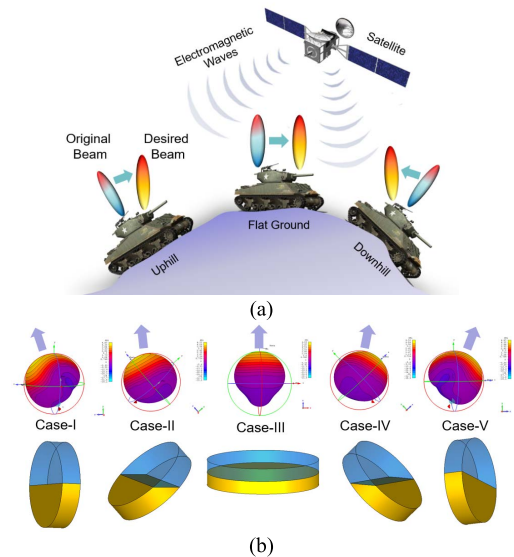

Fig. 2. (a) Illustration of an application scenario of the proposed antenna in a vehicle-mounted satellite communication system. (b) Five different cases for the liquid structures under various topographies and their corresponding radiation patterns.

shown in Fig. 2(a). In a practical scenario, the best signal reception capability is typically achieved when the vehicle moves on a flat ground, which means that the desired antenna beam is identical to the original beam toward 2–3 satellites. However, if the ground is no longer flat, as in the case of the vehicle moving up or downhill, the maximum gain direction of the original antenna beam is not targeted at the direction of the satellite. There will be a significant reduction in the received signal strength, since the satellite signals are not received by the main beam but by the side lobes (with smaller gains) of the antenna. Consequently, the quality of communication is degraded.

In a traditional electrical beam-steering antenna system, when a change in the gyroscopic information or received signal strength indicator (RSSI) is detected, the controller will process the information in accordance with the beam shaping and steering algorithm to determine the phase for each array element. The output signals are sent to the phase and amplitude control circuitry to change the antenna array elements accordingly. Thus, the electrical beam steering for the antenna array is performed to maximize the RSSI and improve the quality of communications. The conventional electrical beam-steering antenna system is very complex, requiring at least three steps—as set out above—to be achieved.

In comparison, the concept of our passive beam-steering liquid antenna system has significant advantages. The most important feature is that there is no need for a detector and a controller to obtain the gyroscopic information and RSSI of the antenna. The antenna beam is automatically steered to the desired direction by the gravitational movement of the immiscible liquid layers as shown in Fig. 2(b). The switching time is fast and the electrical power consumption in traditional systems is eliminated. The five cases shown in Fig. 2(b) illustrate the tilting angle range from +90° to −90°. In practice, the angle range of +60° to −60° could be the most typical scenarios. However, compared with the conventional electrical beam-steering antennas, the antenna beam of the proposed antenna is steered to a fixed direction rather than a flexible direction determined by the electrical beam-steering system.

III. LIQUID MATERIAL CHARACTERIZATION

A. Liquid Selection

It is important to identify suitable liquids when designing the proposed antenna. As mentioned earlier, the bottom dielectric liquid
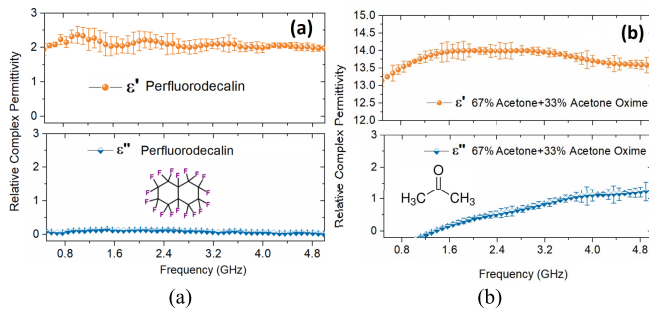
Fig. 3. Measured frequency dependence of the relative complex permittivity of (a) PFD and (b) 67 wt.% acetone/33wt.% acetone oxime mixture. Standard derivation error bars are given.

Fig. 4. Measured frequency dependence of the (a) real part (ε') and (b) imaginary part (ε'') of the relative complex permittivity of acetone and its mixtures with acetone oxime at different concentrations.

Fig. 5. (a) Illustration of the two liquid layers under a flat-ground case (Case-III). (b) 45° tilt (Case-II and Case-IV). (c) 90° tilt (Case-I and Case-V). Potassium permanganate ($KMnO_4$, 3 mg) was added to the low-density top layer to aid visualization. (d) Photograph of the fabricated antenna prototype. The overall dimensions of the antenna prototype are shown as well.

layer is required to have a high density and low permittivity. Having conducted a comprehensive search of the materials, we finally selected perfluorodecalin (PFD), a derivative of decalin in which all of the hydrogen atoms are replaced with fluorine. It is a colorless room temperature liquid, chemically and biologically inert, and stable up to 400 °C. Importantly, it has a very high density of 1.908 g/mL, is chemically inert, and is immiscible with most solvents and dielectric liquids [19]. Thus, PFD is an ideal candidate for the bottom layer liquid resonator, due to its low-loss, low permittivity, high density, and stable properties. The measured relative complex permittivity of PFD is shown in Fig. 3(a). The real part (ε') of the relative complex permittivity (dielectric constant) of PFD is 2–2.2 over a wide frequency range from 0.5 to 5 GHz. The imaginary part (ε'') of the relative permittivity of PFD is very small (<0.05), which means that the dielectric loss tangent ($\varepsilon''/\varepsilon'$) is extremely low.

For the top dielectric liquid layer, we selected a mixture with tunable dielectric constants (in order to achieve configurable antenna resonances) comprising acetone (l) and acetone oxime (s). Acetone is a common colorless solvent that has a melting point of −95 °C, a boiling point of 56 °C, and a density of 0.79 g/mL. Acetone oxime is a white crystalline solid that is highly soluble in many liquids. The relative dielectric constant and density of acetone oxime are ≈ 3 (at 24 °F) and 0.91 g/mL at room temperature, respectively. A tunable relative dielectric constant of ≈ 5 to 20 can be achieved simply by varying the concentration ratio of acetone to acetone oxime. The measured relative complex permittivities of acetone and acetone oxime mixtures at different concentrations are given in Fig. 4(a) and (b).

Fig. 3(b) depicts our selected mixture of acetone/acetone oxime in a 67:33 wt.%, which results in a relative dielectric constant of 14–13.5 over the frequency band of interest. In addition, the dielectric loss of the selected mixture is extremely low. To gain a better understanding of the proposed liquid antenna concept, the images shown in Fig. 5(a)–(c) illustrate the two-layer liquid system under different topological conditions. The selected acetone/acetone oxime mixture was layered onto PFD and artificially dyed using 3 mg of $KMnO_4$ to aid with visualization. As can been seen, the dyes remain solely in the nonperfluorinated layer. Regardless of the orientation of the physical device, the liquid–liquid phase boundary remains constantly flat in relation to the ground due to the effect of differing chemistries, densities, and gravity.

B. Liquid Measurement

The relative complex permittivity of the liquid materials presented in this Communication was measured using an Agilent N9917A FieldFox handheld Microwave Analyzer and a Keysight 85070E Dielectric Probe Kit. All measurements were conducted at room temperature (298 K) under an inert nitrogen atmosphere. The calibration and measurement steps were repeated multiple times to ensure the
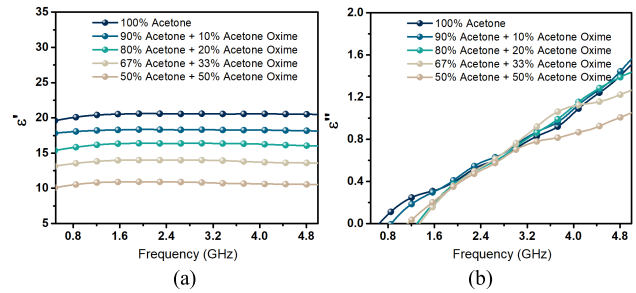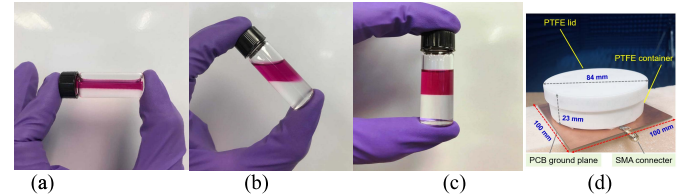
repeatability of data. The standard derivation error bars for a group of 30 measurements of each liquid sample are plotted in Fig. 3. The variations in the results are reasonably small.

IV. ANTENNA PERFORMANCE EVALUATION

A. Numerical Modeling and Simulation

We have designed, fabricated, and tested an example of the proposed liquid antenna that operates at the GPS L1-band around 1.575 GHz using the proposed dielectric liquid resonator. CST Microwave Studio is employed for the simulation. The measured relative complex permittivity of liquids was imported to the CST as new materials under a user-defined dielectric dispersion scheme. Thus, the dielectric loss, conductive loss, and real-time material relaxation were all taken into account to produce highly accurate simulation results.

B. Prototype Fabrication and Measurement

The prototype screw-threaded container was machined to the desired specifications from a single piece of PTFE. The container was filled with the selected liquids and screw sealed by a PTFE lid. The container was pasted to the PCB using double-sided thin foam tape with a thickness of 0.3 mm. A photograph of the fabricated prototype can be found in Fig. 5(d). The overall dimension of the antenna is $100 \times 100 \times 23$ mm^3 which is around $0.52 \times 0.52 \times 0.12$ λ_0^3 at 1.575 GHz.

C. Results and Discussion

As shown in Fig. 6(a), when the antenna is placed on flat ground [Case-III in Fig. 2(b)], two resonant frequency bands (reflection coefficient $S_{11} < -10$ dB) are generated. The first band (B1) covers 1.4–1.8 GHz, while the second band (B2) is located at 2.8–3.55 GHz. The resonances are excited from the fundamental modes in the two liquids of the antenna, namely, the aforementioned $HEM_{11\delta}$ mode of the top-layer liquid resonator of high permittivity and that of the bottom layer PFD resonator with a lower permittivity. The theoretical
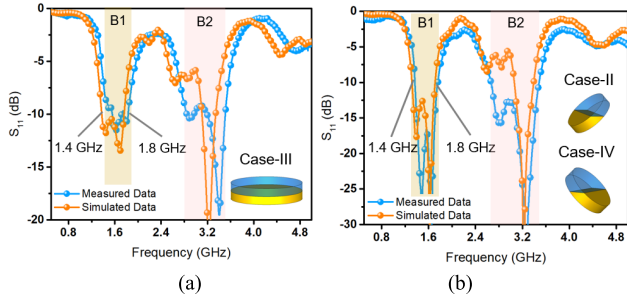
Fig. 6. Simulated and measured reflection coefficients (S_{11}) of the liquid antenna under (a) Case-III (antenna is parallel to flat ground) and (b) Case-IV (antenna is tilted $45°$).
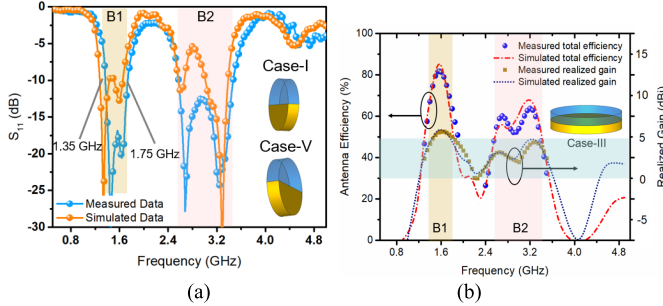

Fig. 7. (a) Simulated and measured reflection coefficients (S_{11}) of the liquid antenna under Case-I and Case-V (antenna is tilted $90°$). (b) Measured and simulated radiation efficiencies and total efficiency of the proposed liquid antenna under Case-III over the frequency band of interest.

resonant frequency of the cylinder DRA at $HEM_{11\delta}$ mode can be calculated using [18]

$$k_0 r = \frac{6.324}{\sqrt{\varepsilon_r + 2}} \left\{ 0.27 + 0.36(x/2) - 0.02(x/2)^2 \right\} \qquad (1)$$

$$k_0 r = \frac{f_{GHz} \cdot h_{cm} \cdot x}{4.7713} \qquad (2)$$

where $x = r/h$, r is the radius of the DR ($r = d_1/2 = 39.5$ mm), h is the height of the DR (9.5 mm for each layer), h_{cm} is the value (without units) of h in centimeters, and ε_r is the relative permittivity of the DR. Using (1) and (2), the theoretical resonant frequencies of the top and bottom cylinder DR layers are around 1.75 and 3.3 GHz, respectively. Therefore, the resonance of B1 is mainly due to the high-permittivity resonator on the top layer. Meanwhile, B2 is originated from the bottom PFD resonator. According to Fig. 6(a), it is also found that the simulated results agree well with the experimental results. The measured S_{11} at 2.8 GHz is smaller than the simulated ones. This could be due to the cable and adapter effects and potential fabrication errors.

Figs. 6(b) and 7(a) show the results for the proposed antenna being physically tilted by $45°$ and $90°$, respectively. In these cases, the position of the feeding slot is changed from the center bottom of the stacked cylinder liquid resonators ($HEM_{11\delta}$ mode) to the edge of two individual semicylinder shapes. The resonant mode is consequently changed to the quasi-$TM_{01\delta}^z$ mode under such conditions [18]. It is known that the $HEM_{11\delta}$ mode of the aperture-fed cylinder DRA could generate a unidirectional broadside radiation, while the $TM_{01\delta}^z$ mode of the same antenna could produce an omnidirectional and conical radiation pattern [18]. The theoretical resonant frequency of the semicylinder DR at $TM_{01\delta}^z$ mode can be obtained as follows:

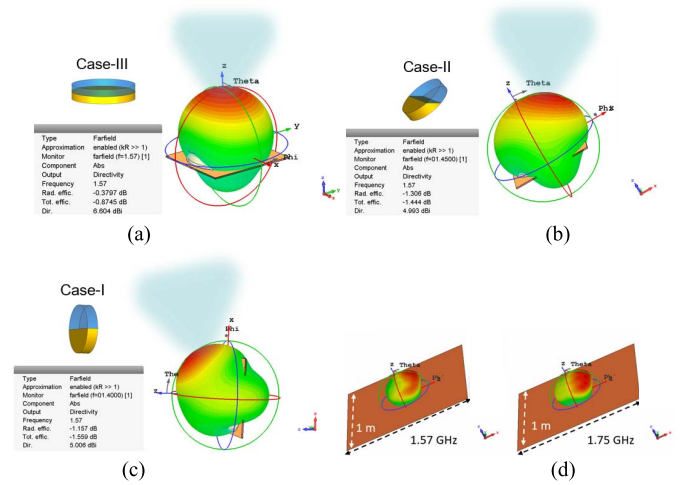$$k_0 r = \frac{\sqrt{3.83^2 + (\pi x/2)^2}}{\sqrt{\varepsilon_r + 2}}. \qquad (3)$$

Fig. 8. 3-D radiation patterns and gains of the proposed antenna at 1.57 GHz under three different cases of tilt. (a) Flat. (b) $45°$ tilt. (c) $90°$ tilt. (d) Radiation patterns at 1.57 and 1.75 GHz when the antenna is mounted on a large metal ground of 1 m $\times$ 1 m.

Using (2) and (3), the resonant frequencies of the semicylinder DRs ($x = 39.5/(2 \times 9.5) = 2.08$) are roughly about 1.55 (high-permittivity DR) and 2.95 GHz (low-permittivity DR). These two resonances are still within the coverage of B1 and B2 bands. It can be seen from Figs. 6(b) and 8(a) that the proposed antenna also covers the band of $\approx$1.4–1.8 (the desired GPS L1 band) and 2.8–3.55 GHz when it is physically tilted. The results are quite comparable with that in Fig. 6(a). It was found that the resonant frequency bands of the antenna were relatively robust regardless of the physical movement, tilt, and rotation of the antenna (in 3-D angles from $-45°$ to $+45°$). Fig. 7(b) shows the simulated and measured antenna efficiencies and realized gains of the proposed liquid antenna under Case-III. It can be seen that the efficiency and gain are up to 83% and 6.6 dBi in B1 and 70% and 4.8 dBi in B2 (not used in GPS), respectively, which shows that the proposed dielectric liquid is of low loss and comparable to traditional DRAs. The average efficiency in B1 is still higher than 76%, demonstrating that the proposed antenna is indeed suitable for wireless satellite communications.

The 3-D radiation patterns of the proposed antenna at three different orientations are depicted in Fig. 8(a)–(c). In order to gain an insightful understanding on the radiation mechanism, the corresponding electric fields (E-field) and magnetic fields (H-field) under these cases are shown as well [see Fig. 9(a)–(c)]. When the antenna is placed on flat ground, it produces a unidirectional radiation beam in its boresight direction (perpendicular to flat ground), as shown in Fig. 8(a). In this case, the maximum gain of the antenna is about 6.6 dBi, while the antenna half-power beamwidth (HPBW) is about $95.4°$. From Fig. 9(a), the contour plot of the E-field shows that it is excited at the bottom feeding slot and propagates to the boresight direction of the antenna through the two layers of the liquid DRA. The H-field is known to be orthogonal to the E-field at any point. As can be seen in Fig. 9(a), the direction of the H-field is rotated along the center near the feeding slot. Thus, if seeing from the top, the E- and H-field distributions of the proposed antenna are comparable with those of the ideal cylinder DRA at $HEM_{11\delta}$ mode.

If the antenna is tilted $45°$, as shown in Fig. 8(b), the radiation pattern is no longer symmetrical. The maximum beam direction is tilted to the direction that is opposite to that of the antenna tilt. In this case, the maximum gain of the antenna is around 4.99 dBi with an HPBW of $117°$. Fig. 8(b) shows that the antenna automatically steers its maximum radiation beam from the antenna boresight to
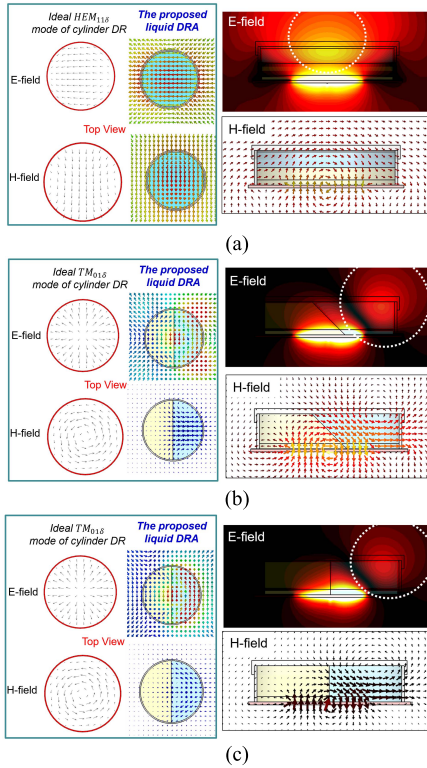
Fig. 9. Simulated contour plots of E-fields and H-fields of the antenna under the three aforementioned cases. (a) Case-III. (b) Case-II and Case-IV. (c) Case-I and Case-V. The field distributions of the ideal $TM_{01\delta}$ and $HEM_{11\delta}$ modes for cylinder DR are presented for comparison (taken from [18]).
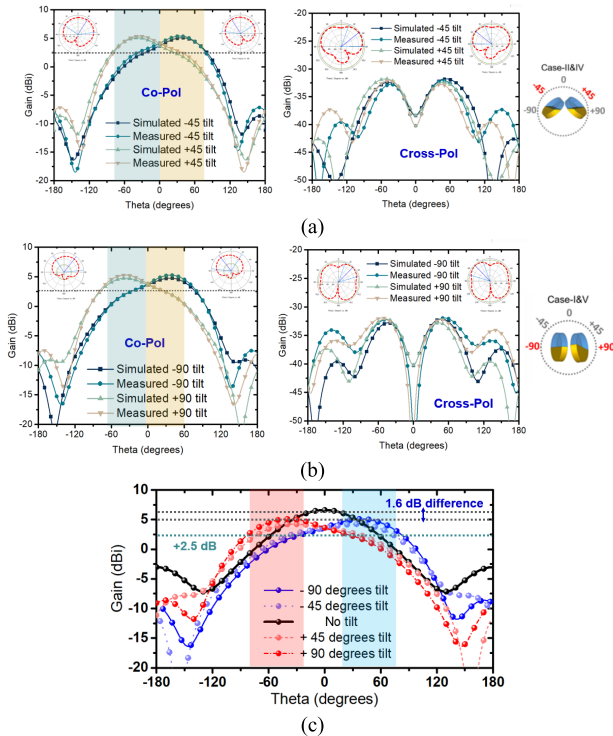

Fig. 10. Simulated and measured E-plane (yoz plane) radiation patterns of the proposed antenna under (a) $\pm45°$ tilt and (b) $\pm90°$ tilt. (c) Simulated E-plane radiation patterns for ±45 and $\pm90°$ physical tilts of the antenna.

the desired direction (perpendicular to flat ground) after the physical movement of the antenna. From the E-field plot, it is demonstrated that the electric field in this scenario does not propagate toward the
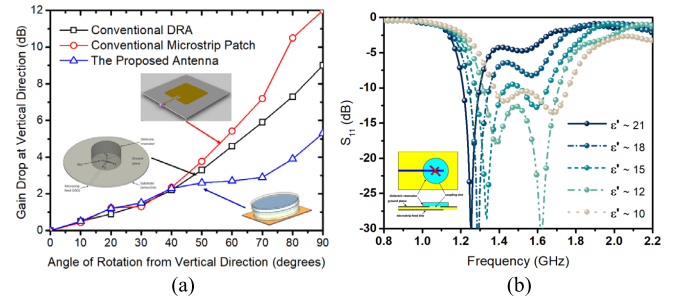

Fig. 11. (a) Comparison of antenna gain drop at the vertical direction during rotation for three different antennas including the proposed antenna and conventional DRA and patch. (b) Tunable resonances of the antenna by using liquids with different relative permittivities in accordance with Fig. 4. An example of crossed slot for CP radiation is given.

boresight direction. The E-field is tilted to the side [see Fig. 9(b)] of the top-layer liquid with a higher relative permittivity. Importantly, the H-field of the antenna is rotated along two centers, one being located at the feeding slot and another found at the side of the high-permittivity liquid resonator. This is significantly different from the H-field in the previous case shown in Fig. 9(a). This might be due to the hybrid quasi-$TM_{01\delta}^z$ mode generation of the two liquid resonators. Compared with the ideal $TM_{01\delta}^z$ mode of cylinder DRA, the E- and H-field distributions of the quasi-$TM_{01\delta}^z$ mode radiation from the two liquid resonators is no longer balanced and symmetrical. In addition, since the high-permittivity liquid is the dominant resonator in B1, the radiation pattern at this band (1.4–1.8 GHz) is, therefore, tilted to the direction of the high-permittivity liquid.

When the antenna is tilted to the direction that is perpendicular to flat ground [see Fig. 8(c)], the radiation pattern of the antenna is also tilted to the desired direction. However, in this case, the maximum radiation beam cannot be perfectly steered to the direction that is orthogonal to the antenna boresight. This is due to the ground plane effect that reflects most of the radiation fields to one direction. The maximum gain of this antenna is around 5 dBi with an HPBW of around 96°. Therefore, the desired beam direction has been covered under such a beamwidth. The antenna can still receive the signals from the satellite once it is tilted 90°. The E-field and H-field results are relatively similar to that of the previous 45° tilt case [see Fig. 9(a) and (b)]. A tilted E-field is produced along the side of the high-permittivity liquid resonator and two rotation centers are observed at the feeding slot and high-permittivity liquid resonator. Fig. 8(d) shows the examples when the antenna is mounted on a large metal ground (such as a car). The antenna beam at 1.57 and 1.75 GHz is switched to the direction that is opposite to the physical tilt. This shows that the desired antenna performance can still be achieved in this scenario.

We also measured the 2-D radiation patterns of the proposed antenna. The E-plane antenna patterns (yoz plane) for $\pm45°$ and $\pm90°$ tilts (Cases I, II, IV, and V) were presented. The E-plane radiation pattern for Case-III could not be measured using our current facilities, since the liquid layer structures would be changed to the structures in accordance with Case-I and Case-V (due to the effect of gravitational force) when the antenna boresight is targeted to the transmitting antenna. The results are presented in Fig. 10. In general, good agreement between the simulated and measured patterns is obtained. The radiation beam of the antenna is passively steered to the desired direction. A comparison of antenna gain drops at the vertical direction when the antenna is tilted from the vertical axis is given in Fig. 11(a) for three different antennas. It can be seen that the proposed antenna is comparable with the conventional DRA

TABLE I
COMPARISON OF THE PROPOSED LIQUID ANTENNA
AND RELATED DESIGNS

Ref. (year)	Fractional bandwidth	Size (λ_0^3)	Beam-steering angle range and maximum realized gain	Number of active components
[2] (2018)	11.54%	1.16 × 1.16 × 0.26	-30° to +30° 9.3 dBi at 5 GHz	2 Need power
[3] (2013)	6.67%	1.21 × 1.90 × 0.03	30° to +30° 9 dBi at 5.1 GHz	24 Need power
[20] (2016)	40%	0.77 × 0.77 × 0.1	N/A 10.5 dBi at 5 GHz	N/A
[21] (2016)	12.4%	0.64 × 0.64 × 0.25	N/A 6 dBi at 1.8 GHz	N/A
This work (2019)	**25%**	**0.52 × 0.52 × 0.12**	**-45° to +45°** **6.6 dBi at 1.57 GHz**	**0** **No power**

λ_0 refers to the free-space wavelength at center frequency.

and microstrip patch antenna when the tilting angle is less than 40°. However, our antenna performs much better than the other antennas when the angle of rotation is greater than 40°. At 70°, the gain drop of our antenna is about 2.5 dB but the conventional DRA and patch antenna gain drops are over 6 dB.

A performance comparison between the proposed antenna and the recent electrical beam-steering antennas [4], [5] and stacked DRAs [20], [21] is given in Table I. It can be seen that our antenna can achieve similar beam-steering angle range without the need for active components and power. The only drawback could be that the steering direction is not flexible. In addition, our antenna has a relatively wide bandwidth and a very small dimension compared with most designs. It is important to note that the design presented is only an example to illustrate the proposed new antenna concept. Other resonant frequency bands can also be achieved by using dielectric liquid resonators with different permittivities. An example of this tunability is presented in Fig. 4. The permittivity data of liquids covering the range of 10–21 can be found. Using liquids in this range results in tunable antenna resonances from 1.2 to 1.8 GHz, which are shown in Fig. 11(b). Moreover, the dimensions of the liquid resonator and PCB can be scaled up or down in order to cover other frequency bands. The feeding slot can be modified to a crossed slot for circular polarization (CP) radiation [18]. An example of such a slot arrangement is presented in Fig. 11(b) as well. This will be our future work since the control of axial ratio versus tilting angle is also a challenging task [17].

V. CONCLUSION

In conclusion, we have introduced and demonstrated a new antenna concept to passively steer the radiation beam to the desired fixed direction by utilizing the liquid fluidity behavior due to gravity. Different from electrical beam-steering antennas and reconfigurable liquid antennas, our proposed design does not require additional phase shifting circuitry, liquid pumps, tunable elements, and their associated electrical power supply. Most importantly, the proposed antenna does not need the detection process of gyroscopic information and RSSI that is essential to determine the desired beam direction in traditional systems. The proposed passive beam-steering liquid antenna exploits gravity to automatically tune the antenna beam to the desired direction for communications. We have theoretically proved and experimentally verified the antenna performance by designing a biphasic liquid–liquid resonator antenna prototype. The detailed results and discussion on the antenna radiation mechanisms, liquid materials selection, and resonant mode control have been presented. This simple, low-cost

antenna concept is highly relevant to wireless communications and radar systems, with potential applications in many important areas such as satellite navigation, mobile communication, and the Internet of Things. The idea offers a new option for the design of beam-steering and reconfigurable antennas.

REFERENCES

[1] C. Liu, S. Xiao, Y.-X. Guo, Y.-Y. Bai, and B.-Z. Wang, "Broadband circularly polarized beam-steering antenna array," *IEEE Trans. Antennas Propag.*, vol. 61, no. 3, pp. 1475–1479, Mar. 2013.
[2] Y. F. Cao and X. Y. Zhang, "A wideband beam-steerable slot antenna using artificial magnetic conductors with simple structure," *IEEE Trans. Antennas Propag.*, vol. 66, no. 4, pp. 1685–1694, Apr. 2018.
[3] P.-Y. Qin, Y. J. Guo, and C. Ding, "A beam switching quasi-Yagi dipole antenna," *IEEE Trans. Antennas Propag.*, vol. 61, no. 10, pp. 4891–4899, Oct. 2013.
[4] W. Aerts, P. Delmotte, and G. A. E. Vandenbosch, "Conceptual study of analog baseband beam forming: Design and measurement of an eight-by-eight phased array," *IEEE Trans. Antennas Propag.*, vol. 57, no. 6, pp. 1667–1672, Jun. 2009.
[5] F. Xiong and R. Romanofsky, "Study of behavior of digital modulations for beam steerable reflectarray antennas," *IEEE Trans. Antennas Propag.*, vol. 53, no. 3, pp. 1083–1097, Mar. 2005.
[6] G. Kahmen and H. Schumacher, "Interactive design of MEMS varactors with high accuracy and application in an ultralow noise MEMS-based RF VCO," *IEEE Trans. Microw. Theory Techn.*, vol. 65, no. 10, pp. 3578–3584, Oct. 2017.
[7] Y. Lu, L. Katehi, and D. Peroulis, "High-power MEMS varactors and impedance tuners for millimeter-wave applications," *IEEE Trans. Microw. Theory Techn.*, vol. 53, no. 11, pp. 3672–3678, Nov. 2005.
[8] I. J. Gupta, I. M. Weiss, and A. W. Morrison, "Desired features of adaptive antenna arrays for GNSS receivers," *Proc. IEEE*, vol. 104, no. 6, pp. 1195–1206, Jun. 2016.
[9] M. Kubo *et al.*, "Stretchable microfluidic radiofrequency antennas," *Adv. Mater.*, vol. 22, no. 25, pp. 2749–2752, Jul. 2010.
[10] J.-H. So, J. Thelen, A. Qusba, G. J. Hayes, G. Lazzi, and M. D. Dickey, "Reversibly deformable and mechanically tunable fluidic antennas," *Adv. Funct. Mater.*, vol. 19, no. 22, pp. 3632–3637, Nov. 2009.
[11] Q. L. Li, S. W. Cheung, D. Wu, and T. I. Yuk, "Optically transparent dual-band MIMO antenna using micro-metal mesh conductive film for WLAN system," *IEEE Antennas Wireless Propag. Lett.*, vol. 16, pp. 920–923, 2017.
[12] C. Hua, Z. Shen, and J. Lu, "High-efficiency sea-water monopole antenna for maritime wireless communications," *IEEE Trans. Antennas Propag.*, vol. 62, no. 12, pp. 5968–5973, Dec. 2014.
[13] J. Sun and K.-M. Luk, "A wideband low cost and optically transparent water patch antenna with omnidirectional conical beam radiation patterns," *IEEE Trans. Antennas Propag.*, vol. 65, no. 9, pp. 4478–4485, Sep. 2017.
[14] L. Xing, Y. Huang, Q. Xu, and S. Alja'afreh, "A transparent dielectric-loaded reconfigurable antenna with a wide tuning range," *IEEE Antennas Wireless Propag. Lett.*, vol. 15, pp. 1630–1633, 2016.
[15] Z. Chen and H. Wong, "Wideband glass and liquid cylindrical dielectric resonator antenna for pattern reconfigurable design," *IEEE Trans. Antennas Propag.*, vol. 65, no. 5, pp. 2157–2164, May 2017.
[16] Z. Chen and H. Wong, "Liquid dielectric resonator antenna with circular polarization reconfigurability," *IEEE Trans. Antennas Propag.*, vol. 66, no. 1, pp. 444–449, Jan. 2018.
[17] C. Song, E. L. Bennett, J. Xiao, A. K. M. Alieldin Luk, and Y. Huang, "Metasurfaced, broadband and circularly polarized liquid antennas using a simple structure," *IEEE Trans. Antennas Propag.*, vol. 67, no. 7, pp. 4907–4913, Jul. 2019.
[18] K. M. Luk and K. W. Leung, Eds., *Dielectric Resonator Antennas*. Bldock, U.K.: Research Studies Press, 2003.
[19] C. Song, E. L. Bennett, J. Xiao, Q. Hua, L. Xing, and Y. Huang, "Compact ultra-wideband monopole antennas using novel liquid loading materials," *IEEE Access*, vol. 7, pp. 49039–49047, 2019.
[20] Y. M. Pan and S. Y. Zheng, "A low-profile stacked dielectric resonator antenna with high-gain and wide bandwidth," *IEEE Antennas Wireless Propag. Lett.*, vol. 15, pp. 68–71, 2016.
[21] M. Zou and J. Pan, "Wide dual-band circularly polarized stacked rectangular dielectric resonator antenna," *IEEE Antennas Wireless Propag. Lett.*, vol. 15, pp. 1140–1143, 2016.